Gjøvik University College

HiGIA
Gjøvik University College Institutional Archive

Please notice:
This is the journal's pdf version.

Detection of worms in error diffusion halftoning

Marius Pedersen[a], Fritz Albregtsen[b] and Jon Yngve Hardeberg[a]

[a]Gjøvik University College, Gjøvik, Norway;
[b]University of Oslo, Oslo, Norway;

ABSTRACT

Digital halftoning is used to reproduce a continuous tone image with a printer. One of these halftoning algorithms, error diffusion, suffers from certain artifacts. One of these artifacts is commonly denoted as worms. We propose a simple measure for detection of worm artifacts. The proposed measure is evaluated by a psychophysical experiment, where 4 images were reproduced using 5 different error diffusion algorithms. The results indicate a high correlation between the predicted worms and perceived worms.

1. INTRODUCTION

Digital halftoning is the process of transforming a continuous tone image to a binary image, to allow printing or displaying on a bi-level display. Many different techniques have been proposed for the transformation. One of these being error diffusion[1] halftoning, its simplicity and ability to produce high quality reproductions has contributed to its popularity. This technique distributes the quantization error along the path of the image scan. This is done by a filter, determining the weight distribution of the error. The original 4 element filter by Floyd and Steinberg[1] resulted in different artifacts.

One of the artifacts produced by error diffusion is worms, where black and white pixels string together are perceived as having a vermicular texture as seen on Figure 1.[2] This artifact is found in the highlights and shadows of the halftoned image. The original filter by Floyd and Steinberg suffers from this artifact, and because of this a number of different error diffusion algorithms have been proposed.

Jarvis et al.[3] proposed a 12 element filter, another 12 element filter was proposed by Stucki,[4] both of these break up worm patterns, but they introduce artifacts in mid-tone areas.[5] Later Fan[6,7] proposed a filter with a long tail, this results in breaking up worm structures in the highlights and shadows while performing similar to the Floyd and Steinberg filter in the mid-tones.[5] An overview of other filters, each with different advantages and disadvantages, is given by Monga et al.[8]

Different approaches to scanning paths have been proposed to create visually more pleasing images. The original Floyd and Steinberg[1] algorithm used a left-to-right scan path, later a serpentine (boustrophedonic) processing was introduced where the scan is left-to-right and then right-to-left (Figure 1). Other more creative paths have been proposed based on space filling curves, as the Peano and Hilbert paths[5] that break up worms, but introduce significant amount of noise.

A number of metrics for halftone quality have been proposed. Lee et al.[9] proposed an image similarity measure to evaluate a hybrid error diffusion algorithm. Veryovka et al.[10] proposed a multiscale approach to analyze edges, and used it to evaluate different halftoning algorithms. Mitsa and Varkur[11] proposed an image quality measure for halftoning based on a spatial filtering of Mean Square Error (MSE). Scheermesser and Bryngdahl[12] proposed a texture metric for halftone images, that find the occurrence or absence of specific textures in quantized images. Nilsson[13] proposed an image quality metric for halftone images that incorporated models of both the printer and observer. S-CIELAB was proposed by Zhang and Wandell[14] as a spatial pre-processor of the CIELAB color difference formulae,[15] and was designed to predict image difference for halftoning, distortion etc.

Even though many measures have been proposed for halftoning, many of them only work on a global scale without having a specific calculation for worms. A specific measure for worms could be used to preserve worms where they are wanted, as in edges, but remove them in areas where they are not wanted. A specific measure for worms could also be used to select the most optimal halftoning algorithm for an image, resulting in the best possible output image. Such a measure for worms could also be included in a toolbox to detect halftoning artifacts.

Contact information: marius.pedersen@hig.no , www.colorlab.no
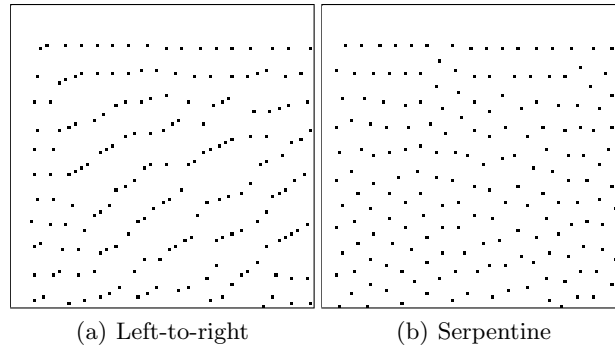
| (a) Left-to-right | (b) Serpentine |

Figure 1. The result of using (a) Floyd and Steinberg left-to-right scan path and (b) Floyd and Steinberg with serpentine scan path. The serpentine scan path breaks up worm patterns, and results in a visually more pleasing image as seen on Figure 1(b).

2. PROPOSED ERROR DIFFUSION WORM MEASURE

This section introduces a measure for worms, called Error Diffusion Worm Measure (EDWM), a multi-step measure as shown in Figure 2. This is a no-reference measure, where no information about the original is used in the calculation.
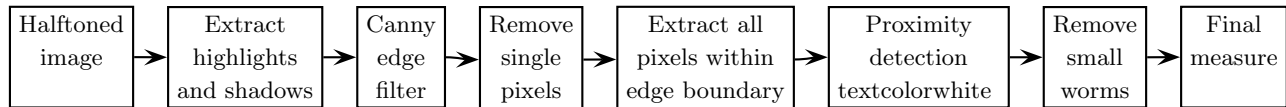

Figure 2. Description of the workflow of the EDWM. Highlights and shadows are extracted from the halftoned image before a Canny edge filter is applied. Single pixels are removed, before all pixels within in the edge boundary are extracted. Then a proximity detection is performed before small worms are removed. The final measure is calculated as the percentage of non-worm pixels divided by the number of pixels in the image.

Since worms are found in highlights and shadows of the image, the halftoned image is filtered to remove parts without highlights and shadows. A sliding filter with width and height of 10 pixels is used, where the mean of each location is found. 10×10 pixels was found to be sufficient to find the information needed to extract highlights and shadows. Thresholds for when a pixel is considered as highlight or shadow is set at 0.15 and 0.85 respectively, on a scale where 0 is where white pixles (no dot of ink placed) are found within the filter and 1 where all pixels are black (a drop of ink). These limits visually gives highlights and shadows. The parts of the halftoned image within the limits (≤ 0.15 and ≥ 0.85 of a grayscale range from 0 to 1) are extracted for further processing.

A Canny edge filter is used to extract edges, where black pixels (a drop of ink) are found next to white pixel areas (no drop of ink), in the image.[16] This filter uses a low and a high threshold for hysteresis, and a sigma as the standard deviation for the Gaussian filter. Pixels placed close together will therefore be identified as forming an edge, and a worm can be thought of as an edge going through the image. Figure 3 shows an example where pixels form a worm, and the Canny filter correctly detects this as an edge. In most cases a sigma of 1, resulting in a 4×4 pixel Gaussian filter, yields good results together with a heuristically choosen pair of thresholds depending on the data. Another advantage of using an edge filter is the fact that worms can be found in both highlights and shadow areas; in the highlights drops of ink make the worms, while in the shadow areas the ink-free areas make the worms. The edge filter does not differentiate between these, just the difference between dark and light areas resulting in a robust method and no special care must be taken if it is in a highlight or shadow area.

In the cases of a single pixel without any connecting pixels the Canny filter will result in an edge around the pixel. A simple filter is applied to remove these single pixels, along with other small pixels not connected to worms. This is done by checking the local neighbourhood around the pixel to identify whether it is connected to other pixels or not, if not connected the pixel is removed and not considered as a part of a worm.
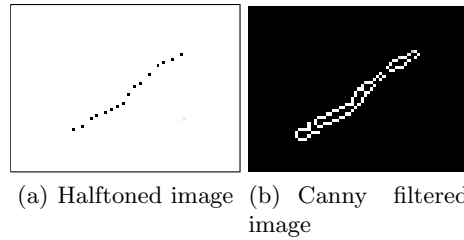
(a) Halftoned image (b) Canny filtered image

Figure 3. Error diffused image and image after Canny egde detection. The Canny egde detection results in a 'shell' around the black pixles.

In order to find the correct pixels that make up the worm the boundary of the object is traced, since this is a binary image a black and white boundary tracing is performed. The exterior of the object is traced along with the boundaries of the holes.

The basis of the worm structure is now found, and the next step of the worm detection is a proximity calculation. The pixels inside a worm are extracted and for each pixel the closest non-worm pixel is located, if this pixel is within a specified distance and angle it is jugded as part of the worm. The angle is based on the angle from the closest detected worm pixel (Figure 4). This process is iterative, so when a pixel is found this pixel is then further checked until all detected pixels are processed. The distance and angle can be set according to the desired sensitivity. Testing has shown that a distance of 50 pixels and angle of 40 degrees gives good results.
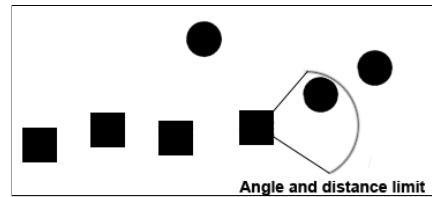

Figure 4. Proximity calculation. Square pixels indicate detected worm pixels. An angle limit and distance limit is set. All non detected pixels (round pixels) inside the limit are found, in this case one pixel is inside both the angle and distance limit. The direction of the angle and distance limit is based on the closest detected pixel, this is done to detect pixels that are linked. The process is iterative and is done until all pixels are processed.

Some small worms have now been detected that observers may not notice,[10] because of this the size of the worm is found by using dilation to increase each pixel. The worms will now "grow" together, and the area of connected dilated pixels is computed. If the area is below a threshold, the pixels are removed from the detected worms.

The final value for the measure is calculated as the percentage of non-worm points divided by the number of pixels in the image. This will result in a value between 0 and 1, where 1 is a worm free image. This normalization will result in the possibility to compare EDWM values across different images. Furthermore the map of worms, computed before the calculation of the final value, can be useful to detect areas where pixels can be rearranged to remove worm artifacts.

3. EVALUATION OF THE EDWM

Evaluation is an important aspect when developing a measure, an experiment was carried out to evaluate the performance of the proposed measure. The performance is measured as the linear correlation against the perceived worms. There are many ways to evaluate halftone quality, and our experiment is inspired by previoues experiments carried out by Mitsa and Varkur,[17] Tontelj et al.[18] and Axelson.[19]

3.1 Experimental setup

Figure 5. Experimental setup. Observers ranked 4 different images reproduced with 5 different error diffusion algorithms.

4 different images were choosen for a psychophysical experiment as seen on Figure 6. One artistic image (Figure 6(b)), with both highlights and shadow areas. One gradient ramp (Figure 6(a)), from white to black. Wang and Parker[20] stated that a gradient ramp is a basic and important evaluation in most halftone evaluations. A gradient will reveal worms, and is often used to demonstrate the performance of error diffusion algorithms.[7, 9, 19, 21–23] One highlight patch (Figure 6(d), 2% black) and one shadow patch (Figure 6(c), 98% black). The highlight and shadow patch are areas where we normally will have worms, and are therefore appropriate images to use.

The images are 600 pixels wide and 200 pixels high, except the artistic image where the height is 450 pixels. These images were reproduced with 5 different error diffusion algorithms, Floyd and Steinberg (FS),[1] Stucki (S),[4] Fan (F),[6, 7] Jarvis, Judice and Ninke (JJN)[3] and Floyd and Steinberg Serpentine (FSS).[5, 24] The images were printed on a HP ColorJet 4600DN on HP Office Paper White (80 g/m^2). The images were printed in 600 DPI simulating 72 DPI.

The experiment was carried out in a dimmed room, with a GretagMacbeth Examolite overhead light source with D50 lighting as seen in Figure 5. The observers were free to move, and no restrictions on viewing distance were given. 12 observers participated in the experiment, males and females.

The experiment was divided into two parts, the first part was to rank the overall quality of the five versions of the image, while the second part was to rank the images according to the amount of worms found in the five versions. Before the second part the observers were taught how to identify worms, and where they occur. This was done to secure reliable data.
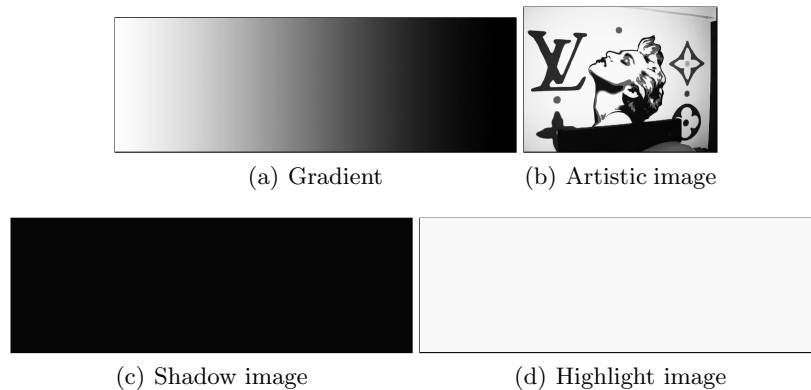

(a) Gradient

(b) Artistic image

(c) Shadow image

(d) Highlight image

Figure 6. The 4 images used in the experiment, surrounded here by a black frame. Each was reproduced with 5 different error diffusion algorithms.

3.2 Results

This section contains results from the psychophysical experiment and EDWM. Analysis of the results are also given. Two types of correlation will be computed for the results, the Pearson product-moment correlation coefficient and the Spearman's rank correlation coefficient.[25] The first assumes that the variables are ordinal, and looks for the linear relationship between variables. The second, Spearman, is a non-parametric measure of correlation that uses the ranks as basis instead of the actual values. This describes the relationship between variables without making any assumptions about the frequency distribution of the variables.

3.2.1 Overall scores

The results from the 12 observers were combined and Z-scores were calculated using Thurstones law of comparative jugdement,[26] the scores were obtained using the Colour Engineering Toolbox.[27] As seen in Figure 7 Floyd and Steinberg Serpentine (FSS) has the highest score both for quality and worms. For the worm artifacts 3 algorithms cannot be differentiated by the observers, Stucki (S), Fan (F) and Jarvis, Judice and Ninke (JJN). The Floyd and Steinberg algorithm (FS) gets the lowest score, and clearly has more worms than the other error diffusion algorithms. In the quality judgement the FS also has the lowest mean Z-score, but cannot be differentiated from S and F. The JJN was rated better than FS, but cannot be differentiated from S and F.

There is also a high correlation between the quality score (Figure 7(a)) and the worm score (Figure 7(b)), the Pearson correlation gives a value of 0.94 (p value: 0.0197). This indicates a strong relationship between the amount of worms and the quality of the image. The images used were choosen based on areas where worms in error diffusion are present. Therefore the conclusion may not be valid in other images with less worms, i.e. without large highlights and shadow areas.
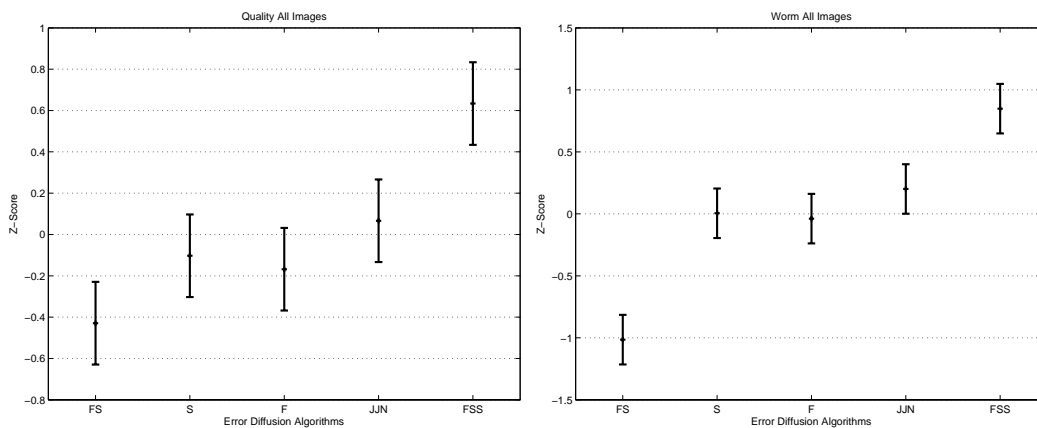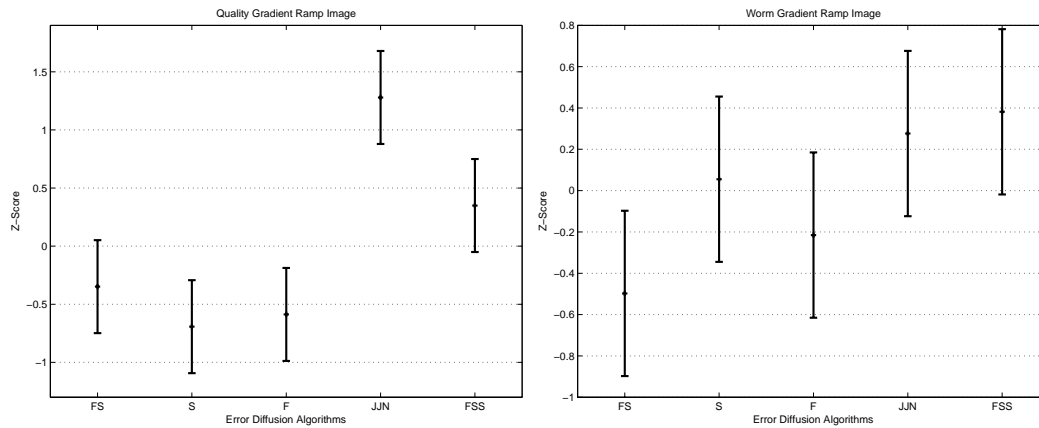

(a) Z-scores for all images based on quality judgement. (b) Z-scores for all images based on worm judgement.

Figure 7. Z-score for quality and worm judgement. From the figures we can see a similarity, indicating that worm artifacts are linked with the quality of error diffused images. The Pearson's correlation gives a value of 0.94 (p value: 0.0197), supporting the similarities found in the figures. We can also notive that in the quality judgement the observers use less of the Z-score scale then in the worm judgement, this indicate that observers agree more on the worm judgement than in the quality judgement.

3.3 Gradient image

Figure 8 and Table 1 shows the results from the psychophysical experiment for the gradient ramp. For the quality judgement (Figure 8(a)) JJN has the best quality, while FSS cannot be differentiated from FS. In the worm judgement (Figure 8(b)), the result is not as clear. FSS can be differentiated from FS, but not from any other algorithms. This also indicates that observers more easily pick one "favorite" algorithm in the quality judgement (Figure 8(a)), while in the worm judgement (Figure 8(b)) the observers do not have a high consensus in ranking. Some observers also indicated that this scene was the hardest to rank, both when it came to quality and worms.

Figure 9 shows a scatter plot of the EDWM and observer scores. FS is correctly given the lowest score by EDWM as the observers did, and FSS is correctly given the highest EDWM score. EDWM has ranked the S before F, the opposite of the observers, but the other error diffusion algorithms are ranked similarly to ranking of the observers. We also see that all points are within a 95% confidence interval. We get a high Pearson correlation, 0.93, indicating that EDWM can predict the amount of perceived worms for this scene.

(a) Z-score for gradient ramp based on quality judgement. (b) Z-score for gradient ramp based on worm judgement.

Figure 8. Z-score for quality and worm judgement for the gradient ramp. In the quality judgement observers agree more on the ranking than in worm jugdement. This is a scene where most observers indicated to have problems with ranking according to worms.

Table 1. Z-scores and EDWM scores for the gradient ramp. We can see that *FSS* has the highest EDWM, i.e. the least worms. *FS* has the lowest value, indicating the most worm artifacts.

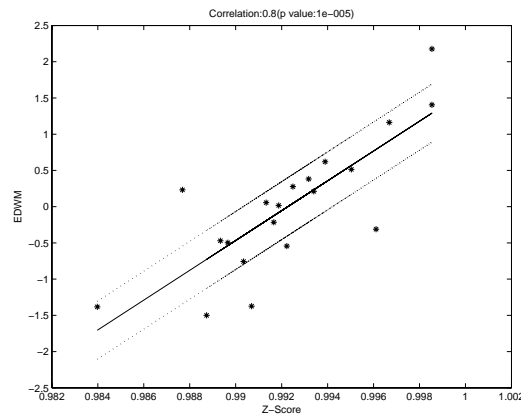| Algorithm	EDWM	Z-score worms
Floyd and Steinberg (*FS*)	0.98965	-0.4975
Fan (*F*)	0.99133	0.0551
Stucki (*S*)	0.99166	-0.2154
Jarvis, Judice and Ninke (*JJN*)	0.99245	0.2763
Floyd and Steinberg Serpentine (*FSS*)	0.99318	0.3815

Figure 9. Correlation for gradient ramp between Z-score and EDWM, plotted with 95% Z-score confidence intervals.

3.4 Artistic image

Figure 10 shows the Z-scores for the artistic image, both for quality (Figure 10(a)) and worm (Figure 10(b)) judgement. For the quality judgement *FSS* cannot be differentiated from *F* and *S* by the observers, but *FSS* was clearly better than *JJN* and *FS*. For the worm judgement *FS* was judged to have more worms than the four other algorithms. These four algorithms gave almost the same amount of worms according to the observers.
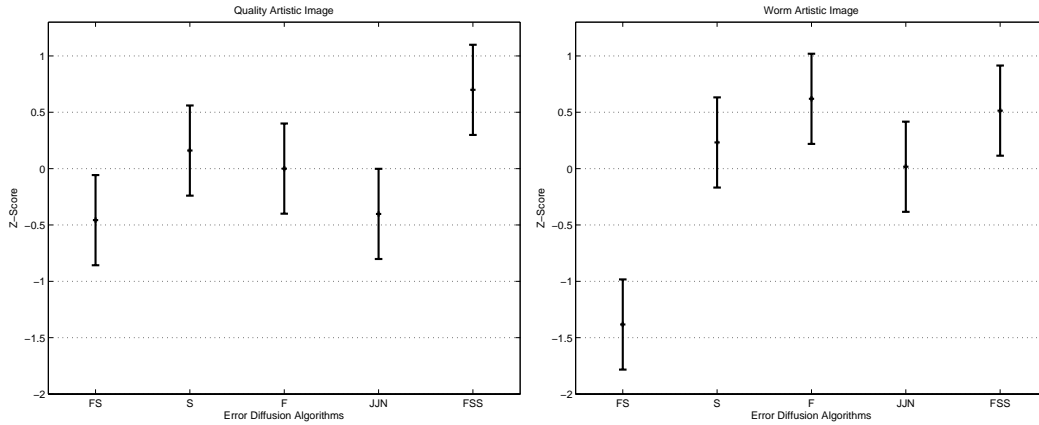
(a) Z-score for artistic image based on quality judgement.

(b) Z-score for artistic image based on worm judgement.

Figure 10. Z-score for quality and worm judgement for the artistic image.

Table 2. Z-score and EDWM scores for the artistic image. *S* has been rated as the error diffusion algorithm with the lowest amount of worms (i.e. best rating by the observers). *FSS* is given the highest EDWM value, but this also has a Z-score close to *S* and cannot be differeniated with a 95% confidence interval.

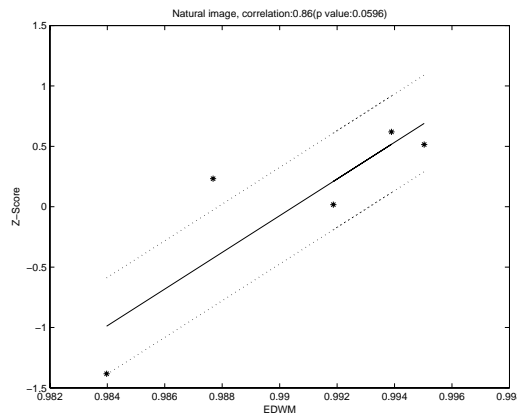| Algorithm	EDWM	Z-score worms
Floyd and Steinberg (*FS*)	0.98398	-1.3830
Fan (*F*)	0.98768	0.2322
Stucki (*S*)	0.99389	0.6196
Jarvis, Judice and Ninke (*JJN*)	0.99187	0.0168
Floyd-Steinberg Serpentine (*FSS*)	0.99503	0.5144

Figure 11. Correlation for artistic image between Z-score and EDWM, plotted with 95% Z-score confidence intervals.

Figure 11 shows a scatter plot of the EDWM and observer score for the artistic image, while data can be found in Table 2. We have a lower correlation than gradient ramp, but still the correlation of 0.86 (*p* value: 0.0596) indicates a strong relation between the predicted worms and perceived worms. Since the EDWM is a no-reference
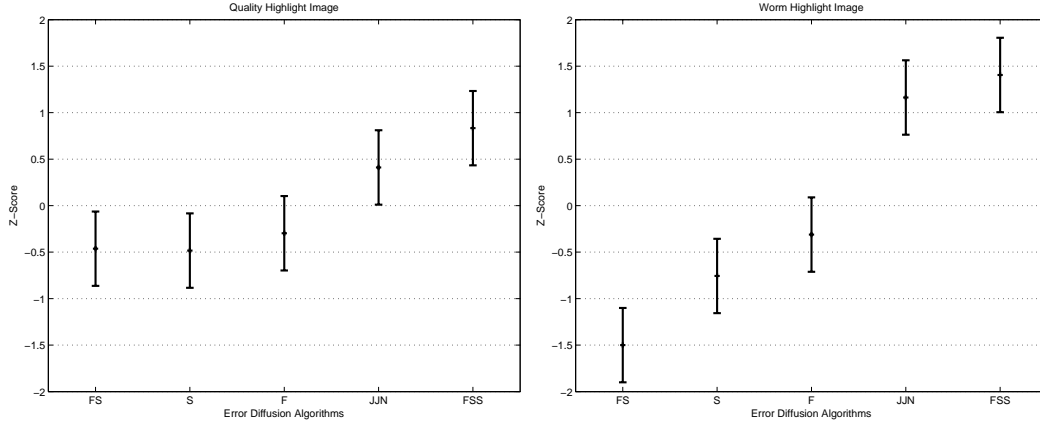
(a) Z-score for highlight image based on quality (b) Z-score for highlight image based on worm judgement.   judgement.

Figure 12. Z-score for quality and worm judgement for the highlight image.

metric, it will not discriminate between worms made by edges in the image and worms in highlight/shadow areas. Because of this EDWM should be used with caution in natural images, because the worms in these images could be wanted in order to reproduce edges. The good correlation found here indicates that EDWM might be used on natural images.

3.5 Highlight image

Figure 12 shows the results for the highlight image regarding quality (Figure 12(a)) and worms (Figure 12(b)), we can see that the ranking is almost similar for the quality and the worm judgement. *FFS* has the same amount of worms and quality as *JJN*, but it can be differentiated from the rest.

Table 3. Z-scores and EDWM scores for the highlight image. *FSS* (Stucki) is given the highest score by the observers, this image also receives the highest EDWM value. We can also see that the ranking of EDWM values and observer scores is the same (Figure 12).

Algorithm	EDWM	Z-score worms
Floyd and Steinberg (*FS*)	0.98873	-1.5002
Fan (*F*)	0.99034	-0.7565
Stucki (*S*)	0.99611	-0.3113
Jarvis, Judice and Ninke (*JJN*)	0.99668	1.1630
Floyd and Steinberg Serpentine (*FSS*)	0.99854	1.4050

Figure 13 shows a scatter plot of the EDWM and observer score for the highlight image. We can see that the ranking of the EDWM values and observer scores is the same (Table 3), indicating that the EDWM is able to correctly rank the images according to perceived worms for this image. We also get a high correlation between the scores, indicating the high performance of EDWM.

3.6 Shadow image

Results for the shadow image are found in Figure 14 and Table 4. *JJN* has the lowest quality judgement (Figure 14(a)) but cannot be differentiated from *FS*. For the worm judgement (Figure 14(b)) *FSS* clearly gave less worms than the four other algorithms. Some observers indicated that this image was the easiest to judge compared to the 3 other images.

Figure 15 shows a scatter plot of the EDWM values and observer score for the shadow image. A correlation of 0.92 (*p* value: 0.0226) indicates a high performance by EDWM.
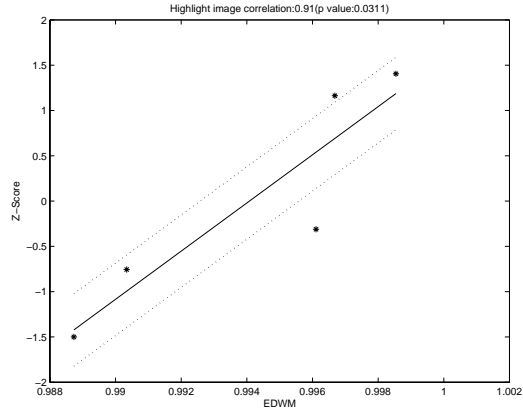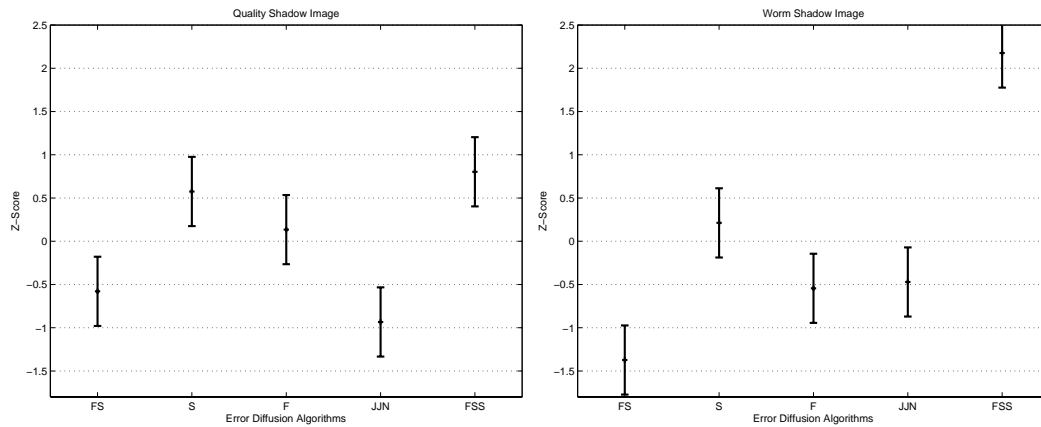
Figure 13. Correlation for highlight image between Z-score and EDWM, plotted with 95% Z-score confidence intervals. We can see that the ranking of the EDWM values and observer scores is the same.

(a) Z-score for shadow image based on quality judgement.

(b) Z-score for shadow image based on worm judgement.

Figure 14. Z-score for quality and worm judgement for the shadow image.

Table 4. Z-scores and EDWM values for the shadow image. *FSS* is the best according to the observers and EDWM.

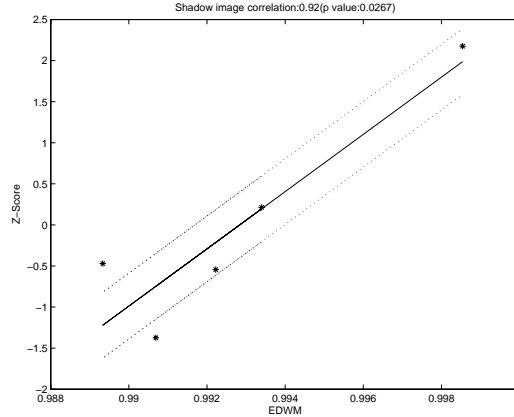| Algorithm	EDWM	Z-score worms
Floyd and Steinberg (*FS*)	0.99069	-1.1752
Fan (*F*)	0.99340	0.2116
Stucki (*S*)	0.99223	-0.5446
Jarvis, Judice and Ninke (*JJN*)	0.98933	-0.4714
Floyd and Steinberg Serpentine (*FSS*)	0.99854	1.9797

Figure 15. Correlation for shadow image between Z-score and EDWM, plotted with 95% Z-score confidence intervals.

3.7 Comparison to other metrics

EDWM's performance is compared against the performance of other metrics. S-CIELAB,[14] Structural Content,[28] Average Distance[28] and MSE have been choosen for comparison. From Table 5 we can see that EDWM outperforms S-CIELAB, Structural Content, Average Distance and MSE as it shows better correlation. All these metrics are full-reference metrics, i.e. they use information from the original image to calculate the difference or quality. The continuous tone image was used as a reference for all metrics. Since EDWM is a no-reference metric, this must be taken into account when analyzing the results, and also the fact that none of the other metrics are specifically made for worm artifacts.

Table 5. Correlation between metric score and Z-score from the worm judgement, with p value in parentheses. Gray cells indicate the best correlation. We can see that EDWM outperforms the other metrics in all images. MSE and Average Distance has a good correlation for the artistic image, but when we look at the p values (AD: 0.2985 and MSE: 0.1241), these are high, indicating that the correlation is by chance.

Metric	Artistic image	Gradient ramp	Highlight image	Shadow image
EDWM	0.86 (0.0596)	0.93 (0.0220)	0.91 (0.0311)	0.92 (0.0226)
S-CIELAB	-0.59 (0.2906)	0.07 (0.9143)	-0.48 (0.4106)	0.64 (0.2500)
Structural Content	0.08 (0.8948)	-0.09 (0.8836)	-0.23 (0.7149)	-0.15 (0.822)
Average Distance	-0.59 (0.2985)	-0.19 (0.7550)	-0.23 (0.7148)	-0.15 (0.8206)
MSE	-0.77 (0.1241)	-0.17 (0.7884)	-0.23 (0.7148)	0.15 (0.8206)

3.7.1 Overall performance

Since the results from EDWM are normalized we can compare results obtained for different images. Figure 16 shows the correlation between Z-scores from the worm judgement for all images and EDWM values for all images (Tables 1 - 4). We can see a clear relationship between the Z-scores and EDWM values, this is also confirmed by a Pearson correlation of 0.81 (p value: 1e-005). Compared to the other metrics EDWM is significantly better (Table 6). The other measures have a very low correlation, this is because they have big differences in the values between images, resulting in a correlation close to 0.[29] Our measure also has the highest Spearman correlation, indicating that the ranking from it corresponds to the ranking made by the observers.

4. CONCLUSION AND FURTHER RESEARCH

A measure for worms, EDWM, has been proposed. The measure is simple to compute, and does not require any information about the original image. It also allows for comparison of results across different images, resulting in a robust measure. A psychophysical experiment was carried out to evaluate the performance of EDWM, and the results indicate a high performance. EDWM also clearly outperforms other metrics.
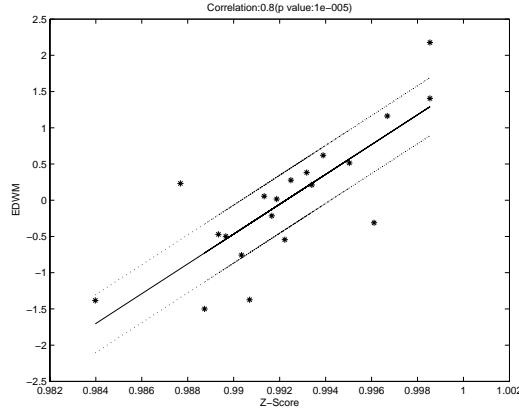
Figure 16. Correlation between all Z-score from worm judgement and all EDWM values, plotted with 95% confidence intervals. From the figure we can see a strong correlation (Pearson correlation of 0.81, p value: 1e-005). The calculated Spearman correlation is 0.77 (p value 0.0001), indicating a correct ranking of predicted worms according to the observer ranking.

Table 6. Correlation between metric score and Z-scores from the worm judgement for all images, with p values in parentheses. We can see that EDWM outperforms the other metrics in all images with a correlation of 0.81 (p value: 1e-005), and the Spearman correlation of EDWM is also higher than for the other metrics. The other measures have a very low correlation due to big differences in the results between the images. Gray cells indicate the best correlation.

Metric	Pearson correlation	Spearman correlation
EDWM	0.81 (1e-005)	0.77 (0.0001)
S-CIELAB	0.01 (0.9715)	0.06 (0.7967)
Structural Content	0.00 (0.9876)	-0.12 (0.6267)
Average Distance	0.00 (0.9945)	0.00 (0.9849)
MSE	-0.02 (0.9451)	0.06 (0.7888)

Since EDWM is a no-reference metric it could detect worms in an image where worms are needed in order to reproduce an edge. An extension of EDWM to a reference metric could solve this problem and make EDWM more robust for use in artistic images. One way to improve and extend EDWM could be to decrease the angle limit in the proximity detection as more co-linear pixels are detected.

5. ACKNOWLEDGEMENTS

REFERENCES

[1] Floyd, R. and Steinberg, L., "An adaptive algorithm for spatial grayscale," in [*Proceedings of the Society for Information Displays*], **17**(2), 75–77 (1976).

[2] Spaulding, K. E., Couwenhoven, D. W., and Miller, R., "Improved error diffusion incorporating a visual model," in [*Human Vision and Electronic Imaging III*], Rogowitx, B. E. and Pappas, T. N., eds., **3299**, 452–460, SPIE (jul 1988).

[3] Jarvis, J., Judice, C., and Hinke, W., "A survey of techniques for the display of continuous tone pictures on bilevel display," *Computer Graphics and Image Processing* **5**, 13–40 (1976).

[4] Stucki, P., "Mecca - a multiple error correcting computation algorithm for bi-level image hard copy reproduction," tech. rep., IBM research laboratory, Zurich, Switzerland (1981).

[5] Lau, D. L. and Arce, G. R., [*Modern Digital Halftoning*], Dekker (2000).

[6] Fan, Z., "A simple modification of error-diffusion weights," in [*Proceedings of SPIE*], (1992).

[7] Shiau, J. and Fan, Z., "A set of easily implementable coefficients in error diffusion with reduced worm artfacts," in [*Color imaging: device-independent color, color hardcopy, and graphic arts*], **2658**, 222–225, SPIE (1996).

[8] Monga, V., Damera-Venkata, N., and Evans, B. L., "Image halftoning by error diffusion: A survey of methods for artifact reduction." www.ece.utexas.edu 28/07/08 (2003).

[9] Lee, J., Horiuchi, T., Saito, R., and Kotera, H., "Digital color image halftone: Hybrid error diffusion using the mask perturbation and quality verification," *The Journal of Imaging Science and Technology* **51**, 391–401 (September/October 2007).

[10] Veryovka, O., Fournier, A., and Buchanan, J. W., "Multiscale edge analysis of halftoned images," in [*Proc. SPIE, Human Vision and Electronic Imaging III*], Rogowitz, B. E. and Pappas, T. N., eds., **3299**, 461–472, SPIE, San Jose, CA, USA (Jan 1998).

[11] Mitsa, T. and Varkur, K., "Evaluation of contrast sensitivity functions for the formulation of quality measures incorporated in halftoning algorithms.," in [*Proc. IEEE Int. Conf. Acostics, speech, signal processing*], **3**, 313–316 (1992).

[12] Scheermesser, T. and Bryngdahl, O., "Texture metric of halftone images," *J. Opt. Soc. Am. A* **13**, 18–24 (1996).

[13] Nilsson, F., "Objective quality measures for halftoned images," *Journal of Optical Society of America* **16**, 2151–2162 (1999).

[14] Zhang, X. and Wandell, B. A., "A spatial extension of CIELAB for digital color image reproduction," in [*Soc. Inform. Display 96 Digest*], *Proc. Soc. Inform. Display 96 Digest* , 731–734 (1996).

[15] Commission Internationale de l'E´clairage CIE, "Colorimetry, 2nd ed.publication cie 15.2, bureau central de la CIE," (1986).

[16] Canny, J., "A computational approach to edge detection," *IEEE Transactions on Pattern Analysis and Machine Intelligence* **8**(6), 679–698 (1986).

[17] Mitsa, T. and Varkur, K., "Evaluation of contrast sensitivity functions for the formulation of quality measures incorporated in halftoning algorithms," in [*IEEE Int. Conference on Acoustics, Speech and Signal Processing*], **5**, 301–304 (Apr 1993).

[18] Trontelj, H., Farrell, J. E., Wiseman, J., and Shur, J., "Optimal halftoning algorithm depends on printing resolution," *SID Digest* , 749–752 (1992).

[19] Axelson, P.-E., *Quality Measures of Halftoned Images*, Master's thesis, Linköping University (2003).

[20] Wang, M. and Parker, K. J., "Prediction of the texture visibility of color halftone patterns," *Journal of Electronic Imaging* **11**, 195 – 205 (April 2002).

[21] Scheermesser, T. and Bryngdahl, O., "Spatially dependent texture analysis and control in digital halftoning," *J. Opt. Soc. Am. A* **14**, 827–835 (1997).

[22] Pappas, T. N. and Neuhoff, D. L., "Least-squares model-based halftoning.," *IEEE Transactions on Image Processing* **8**(8), 1102–1116 (1999).

[23] Kolpatzik, B. and Bouman, C., "Optimized error diffusion for high-quality image display," *Journal of Electronic Imaging* **1**, 277–292 (Jul 1992).

[24] Ulichney, R., [*Digital halftoning*], MIT Press (1987).

[25] Kendall, M. G., Stuart, A., and Ord, J. K., [*Kendall's Advanced Theory of Statistics: Classical inference and relationship*], vol. 2, A Hodder Arnold Publication, 5 ed. (1991).

[26] Thurstone, L. L., "A law of comparative judgment," *Psychological Review* **34**, 237 (1927).

[27] Green, P. and MacDonald, L., eds., [*Colour Engineering: Achieving Device Independent Colour*], John Wiley & Sons (2002).

[28] Eskicioglu, A., Fisher, P., and Chen, S., "Image quality measures and their performance," in [*IEEE Transactions on Communications*], **43**, 2959–2965 (Dec 1995).

[29] Pedersen, M. and Hardeberg, J. Y., "Rank order and image difference metrics," in [*CGIV 2008 Fourth European Conference on Color in Graphics, Imaging and Vision*], IS&T, Terrassa, Spain (Jun 2008).